Contact force–displacement laws and the mechanical behavior of random packs of identical spheres

David Elata [*], James G. Berryman

Earth Sciences Division, Lawrence Livermore National Laboratory, P.O. Box 808, Livermore, CA 94551, USA

Abstract

The contact force–displacement law of two identical elastic spheres can independently display: nonlinear response, path dependence and dissipation due to slip. Omitting relative roll and torsion between the two spheres, a general contact force-displacement law is derived analytically by integrating the differential form of the Hertz–Mindlin solution along the contact displacement path. The Hertz–Mindlin contact law and a different contact law formulated by K. Walton are special cases of this general contact law. Implementation of the contact law in numerical codes may be cumbersome because it requires a full description of the contact load history. Some simplified contact force-displacement laws proposed in the literature that overcome this difficulty are shown to be thermodynamically inconsistent (i.e., unphysical) since they permit energy generation at no cost. The mean-field approximation and statistical averaging for calculating macroscopic stress–strain relations are discussed with respect to various contact force–displacement laws.

Keywords: Contact mechanics; Granular material

1. Introduction

The mechanical properties of brittle granular materials, such as sands and poorly consolidated rocks, are strongly affected by local intergranular effects. These granular materials are often modeled by representing their geometry as a close random pack of elastic spheres, formulating a contact force–displacement law that relates the contact force acting between two spheres to their relative displacement, and

defining an averaging scheme to obtain the macroscopic response. The contact force–displacement law of two elastic spheres can independently display: nonlinear response, path dependence, and dissipation due to slip. These effects are evident even when the spheres are linearly elastic and the relative displacements are small. Disregarding relative roll and torsion between two spheres in contact, the general contact law is derived analytically in Section 2 by integrating the differential form of the Hertz–Mindlin solution along the contact displacement path (Elata, 1996). The Hertz–Mindlin contact law (Mindlin, 1949) and an alternative contact law formulated by Walton (1978) are special cases of this general contact law. The contact law deals differently with increasing and decreasing normal contact

* Corresponding author. Present address: Faculty of Mechanical Engineering, Technion-Israel Institute of Technology, Haifa 32000, Israel. Tel.: +972-4-8293184; fax: +972-4-8324533; e-mail: elata@tx.technion.ac.il

displacements, and it is shown that the tangential contact traction at any point along the loading path depends only on a *selective part of the load history* (Johnson and Norris, 1996a).

Implementation of the contact law in numerical codes may be cumbersome because it requires a full description of the contact load history. This difficulty may be overcome by using some simplified contact force–displacement relations proposed in the literature. In Section 3, some of these simplified contact laws are shown to be *thermodynamically inconsistent* (i.e., unphysical) since they permit energy generation at no cost, while other simplified contact laws achieve thermodynamical consistency by overestimating the mechanical dissipation.

Section 4 considers the mean-field approximation and statistical averaging schemes that are used to calculate the macroscopic stress–strain relations. The effect of approximating the contact force–displacement law on these stress–strain relations is discussed.

2. Contact problem for two spheres

Consider two identical spheres in contact (Fig. 1). Both spheres having radius R are composed of a linear elastic material with Poisson ratio ν and shear modulus μ. The centers of the spheres are displaced axially (u_n) and tangentially (u_t) as illustrated in Fig. 1, in a way that precludes any relative roll or torsion between them. Due to the symmetry of the problem, the normal and tangential displacements of the center of the contact area with respect to the center of either spheres will be equal to u_n and u_t, respectively. Hence, throughout this discussion, u_n
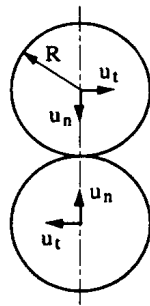

Fig. 1. The contact between two identical elastic spheres.

and u_t will be referred to as the normal and tangential contact displacements.

2.1. Increasing normal contact displacement

Hertz solved the contact problem of two identical elastic spheres axially pressed together (Johnson, 1985), and showed that the normal traction in the circular contact area is given by

$$q_n = \frac{4\mu}{\pi R(1 - \nu)} \left(Ru_n - r^2 \right)^{1/2}, \tag{1}$$

where r $(0 \le r \le \sqrt{Ru_n})$ is the radial distance from the center of the contact area. Mindlin (1949) showed that when the two axially pressed spheres are further displaced tangentially, the contact area and the normal traction distribution are unaffected and the axisymmetric tangential traction is given by

$$q_t = \frac{4\mu u_t}{\pi(2 - \nu)} \left(Ru_n - r^2 \right)^{-1/2}. \tag{2}$$

This solution assumes that *no relative roll or torsion* occurs between the spheres. The tangential traction is singular at the circumference of the contact, where the normal traction vanishes. Accordingly, the possibility of slip must be taken into account (Mindlin, 1949; Mindlin and Deresiewicz, 1953).

An important solution showing that a relative tangential displacement u_t does not necessarily cause slip was presented by K. Walton (1978), who considered the special case with the normal and tangential contact displacements applied simultaneously and proportionally so that

$$\frac{u_t}{u_n} = c = \text{constant}. \tag{3}$$

The resulting tangential and normal tractions for this case are given by

$$q_n = \frac{4\mu}{\pi R(1 - \nu)} \left(Ru_n - r^2 \right)^{1/2}. \tag{4}$$

$$q_t = \frac{8\mu c}{\pi R(2 - \nu)} \left(Ru_n - r^2 \right)^{1/2}. \tag{5}$$

In contrast to the Hertz–Mindlin solution, these tangential and normal tractions are proportional and consequently, slip occurs over the entire contact area or does not occur at all (Walton, 1978).

The difference between the Hertz–Mindlin and Walton solutions is a result of the difference in the specific loading path considered in each case. In order to consider general arbitrary loading paths, the differential form of the Hertz–Mindlin traction–displacement relation is written as

$$dq_n = \frac{2\mu}{\pi(1-\nu)}\left(Ru_n - r^2\right)^{-1/2}du_n. \tag{6}$$

$$dq_t = \frac{4\mu}{\pi(2-\nu)}\left(Ru_n - r^2\right)^{-1/2}du_t$$

$$= \frac{4\mu}{\pi(2-\nu)}\left(Ru_n - r^2\right)^{-1/2}C(\tau)du_n, \tag{7}$$

where dq_n and dq_t are the normal and tangential traction differences, du_n and du_t are the normal and tangential contact displacement differences, dq_t results from an applied tangential displacement change du_t while keeping u_n fixed, and $C(\tau)$ is the ratio between tangential and normal displacement differences

$$C(\tau) = \frac{du_t}{du_n}. \tag{8}$$

Here τ is a loading history parameter (e.g., time) and it is understood that u_n and u_t are parametric functions of τ. Notice that, although dq_t and dq_n are singular at the circumference of the contact area, their ratio is a (bounded) linear function of $C(\tau)$. By integrating Eqs. (6) and (7) over the appropriate loading paths, both the Hertz–Mindlin and the Walton traction–displacement relations may be derived (Elata, 1996).

For any given state along the loading path, the tractions may be integrated over the contact area to give the contact force–displacement law

$$f_n = \int_A q_n(u_n)\,dA = \frac{8}{3}\frac{\mu}{1-\nu}R^{1/2}u_n^{3/2}, \tag{9}$$

$$f_t = \int_A \int_{\text{load path}} dq_t(u_n(\tau), C(\tau))\,dA. \tag{10}$$

The normal and tangential contact stiffnesses are given by

$$k_n = \frac{df_n}{du_n} = \frac{4\mu}{1-\nu}R^{1/2}u_n^{1/2}, \tag{11}$$

$$k_t = \frac{\partial f_t}{\partial u_t}\bigg|_{u_n} = \frac{8\mu}{2-\nu}R^{1/2}u_n^{1/2}, \tag{12}$$

where k_t is obtained by taking the partial derivative of f_t with respect to u_t while keeping u_n fixed. Also notice that both cross partial derivatives vanish, i.e.,

$$\frac{\partial f_n}{\partial u_t}\bigg|_{u_n} = 0, \quad \frac{\partial f_t}{\partial u_n}\bigg|_{u_t} = 0.$$

The stiffnesses defined in Eqs. (11) and (12) are functions of the current value of u_n only, and are independent of the loading path history.

In order to demonstrate the path dependence of the contact tractions, consider three loading paths ending with the same contact displacement. The paths and the resulting normal and tangential contact tractions are qualitatively described in Table 1. Notice that the resulting normal traction is identical for all three paths but the tangential traction is different. Consequently, the resulting normal contact force f_n will also be identical for all three paths but the resulting tangential contact force f_t will be different. In this respect, it should be emphasized that none of these paths necessarily involve slip [even though the tangential traction for path (c) resembles the slip-induced distribution calculated by Mindlin and Deresiewicz (1953, see their Fig. 1)].

2.2. Decreasing normal contact displacement.

Along loading/unloading paths that include a decrease of normal displacement, slip may occur. By way of illustration, consider a contact loaded as in

Table 1
Various contact load paths and their resulting normal and tangential contact tractions.

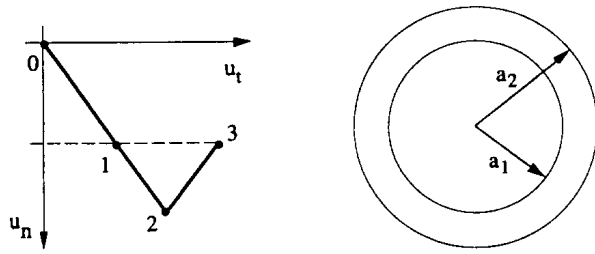| load path	(a)	(b)	(c)
qualitative normal traction distribution q_n			
qualitative tangential traction distribution q_t			

Fig. 2. A contact displacement path and the related contact area. Points 1 and 3 have the same normal displacement and therefore have the same contact area with radius a_1. Point 2 has a larger normal displacement and therefore has a larger contact area with radius $a_2 > a_1$ ($u_n = 0$ is associated with a point contact).

Fig. 3. Contact displacement load path.

path 0–1–2 (Fig. 2a) to a point where the normal and tangential tractions are non-zero, and assume that the spheres are sufficiently rough so that no slip occurs during this loading. In the next path segment 2–3, by reducing the normal displacement from point 2 to 3 ($u_{n3} = u_{n1}$), the radius of the contact area is reduced (Fig. 2b) from $a_2 = \sqrt{Ru_{n2}}$ to $a_1 = \sqrt{Ru_{n1}}$, freeing an annulus ($a_1 \le r \le a_2$) of its tractions. Consequently, the contact has lost all previous information of all states for which $u_n > u_{n1}$, and the tractions at point 3 are therefore the same as if the contact was loaded along the path 0–1–3 (Johnson and Norris, 1996a). Another example is the load path described by the solid line in Fig. 3. The contact traction at point 1' is the same that would result by following the dashed line from point 1 to 1' (rather than following the solid line), and the contact traction at point 3 is the same that would result by taking the direct path from point 2 to point 2' along the dotted line and then continuing along the solid line to point 3. The general rule is that any load path segment connecting two points of equal normal displacement $u_n = \tilde{u}_n$, between which the normal displacement is greater than or equal to $\tilde{u}_n$, can be replaced with a constant normal displacement path $u_n = \tilde{u}_n$ (this applies only to current or previous points along the load path, not future points, even if their normal displacement will be smaller than $\tilde{u}_n$). In this constant normal displacement path, the tangential tractions tend to become singular and slip will occur [Eq. (7)].

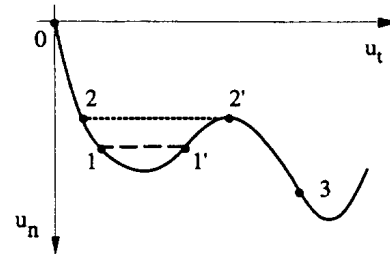Summarizing this discussion, the contact tractions at any given state ($u_n(\tau_1)$, $u_t(\tau_1)$) may be calculated

by integrating the differential form of the Hertz–Mindlin Eqs. (6) and (7) along the loading path while:

(i) replacing the time history of $u_n(\tau)$ with $\tilde{u}_n(\tau, \tau_1)$ where

$$\tilde{u}_n(\tau, \tau_1) = \inf u_n(\theta) \text{ for } \tau \le \theta \le \tau_1, \qquad (13)$$

(ii) continuously limiting the magnitude of the tangential traction q_t with the friction threshold $\mu_f q_n$, where μ_f is the surface friction coefficient.

Mindlin and Deresiewicz (1953, Section 10) also predict that slip occurs when u_n is decreased, however it is important to note that not every decrease of normal contact displacement involves slip. As a simple example, consider unloading from point 2 in Fig. 2 back to point 1 retracing the load path. In this case no slip occurs and moreover, as long as the contact displacements maintain their proportionality, the contact tractions are determined by the contact law formulated by Walton (1978) [Eqs. (4) and (5) here]. Another example is decreasing the normal contact displacement from point 2 of load path (a) described in Table 1. Unloading along the segment 2–1, the tangential force remains constant and no slip occurs.

The discussion in this and the following sections is not general in the sense that the tangential displacements and tractions are required to maintain their orientation within the contact plane. In the more general case of the contact problem considered here, the orientation of the tangential displacements and tractions may change continuously within the contact plane. However, the added complexity needed to allow this degree of generality is technical, and for simplicity the discussion and examples in this manuscript are limited to a fixed orientation of tangential displacements and tractions.

3. Simplified contact force–displacement laws

Implementation of the contact law described in Section 2 in numerical codes may be cumbersome because it requires a complete description of the contact load history. In order to facilitate simulations, some simplified contact force–displacement laws have been proposed in literature. One possible simplification is achieved by ignoring path dependence when the ratio between the tangential and normal contact forces is smaller than a surface friction coefficient μ_f (e.g., Jenkins and Strack, 1993)

$$f_n = \frac{8}{3}\frac{\mu}{1-\nu}R^{1/2}u_n^{3/2}, \tag{14}$$

$$f_t = \begin{cases} f_t^* & \text{for } |f_t^*| \le f_n\,\mu_f & (15a) \\ \text{sign}(f_t^*)f_n\,\mu_f & \text{for } |f_t^*| > f_n\,\mu_f & (15b) \end{cases}$$

where

$$f_t^* = 8\frac{\mu}{2-\nu}R^{1/2}u_n^{1/2}u_t. \tag{16}$$

For cases in which the condition in Eq. (15b) is satisfied, slip is assumed to occur over the entire contact and the resulting contact force–displacement law is path dependent. In contrast, for cases in which the condition in Eq. (15a) is satisfied, the resulting contact force–displacement law is path independent. To demonstrate the thermodynamic implications of this contact force–displacement law, consider the two cyclic loading paths described in Fig. 4. The contact displacements, the forces, and the work done by these forces are illustrated in Fig. 5, for the arbitrary values [1].

$$\nu = 0.25, \tag{17a}$$

$$\mu_f = 1.0, \tag{17b}$$

$$u_{n1} = R(3/8)^{2/3}, \tag{17c}$$

$$u_{n3} = R(3/4)^{2/3}, \tag{17d}$$

$$u_{t3} = \frac{R}{8}\frac{2-\nu}{1-\nu}\frac{1}{\sqrt{u_{n1}}}, \tag{17e}$$

which have been chosen to ensure that the condition in Eq. (15a) is satisfied. As can be seen in Fig. 5, both cycles begin and end in a stress free state and therefore, in both cycles no strain energy is stored in
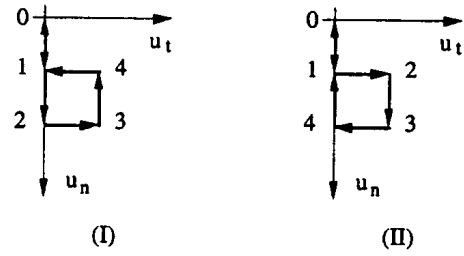

Fig. 4. Two possible contact displacement cycles.

the spheres. For both cycles, the net work done by the normal force is zero. In contrast, the net work done by the tangential force in cycle (I) is greater than zero. It is tempting to attribute this net work to frictional dissipation but as can be seen, the net work done in the reverse cycle (II) has the same absolute value but a negative sign. In other words, the contact force–displacement law (14)–(16) is thermodynamically inconsistent (i.e., unphysical) in the sense that it allows energy generation at no cost.

Another simplified contact force–displacement law relates the tangential force and tangential displacement in a differential form (e.g., Chang et al., 1992)

$$f_n = \frac{8}{3}\frac{\mu}{1-\nu}R^{1/2}u_n^{3/2}, \tag{18}$$

$$f_t = \begin{cases} f_t^* & \text{for } |f_t^*| < f_n\,\mu_f & (19a) \\ \text{sign}(f_t^*)f_n\,\mu_f & \text{for } |f_t^*| \ge f_n\,\mu_f, & (19b) \end{cases}$$

where f_t^* is the solution of the differential equation

$$\mathrm{d}f_t^* = \frac{16}{3}\frac{\mu}{2-\nu}R^{1/2}u_n^{1/2}\left(1-\frac{f_t^*}{f_n\,\mu_f}\right)^{1/3}\mathrm{d}u_t. \tag{20}$$

In contrast to Eqs. (14)–(16), this contact force–displacement law allows the tangential force to remain constant when the normal contact displacement is increased while keeping the tangential displacement fixed. However, when the condition in Eq. (19a) is satisfied, the resulting contact force–displacement law fails to describe possible reduction of the contact tangential force due to reduction of the normal contact displacement (reduction of contact area). To demonstrate the thermodynamic implication of this, consider the two load paths described in Fig. 4. The contact displacements, forces Eqs. (18)–(20) and work done by these forces [Eq. (20) can be

solved analytically for a given path], are illustrated in Fig. 6 for the arbitrary values (see footnote [1]),

$$\nu = 0.25, \tag{21a}$$

$$\mu_f = 1.0, \tag{21b}$$

$$u_{n1} = R(3/8)^{2/3}, \tag{21c}$$

$$u_{n3} = R(3/4)^{2/3}, \tag{21d}$$

---

[1] The magnitude of the contact displacements is clearly to large to be considered elastic, however this does not affect the quantitative conclusions of this section.

$$u_{t3} = R\tfrac{7}{16}3^{2/3}(2^{2/3} - 1), \tag{21e}$$

which have been chosen to ensure that the condition in Eq. (19a) is satisfied whenever u_t is changing [i.e., the work done by the tangential contact force is unaffected by any slip arising from Eq. (19b)]. As can be seen in Fig. 6, both cycles begin and end in a stress free state and therefore, in both cycles no strain energy is stored in the spheres. For both cycles the net work done by the normal force is zero. In cycle (II) the net work done by the tangential force is greater than zero, but the net work done in the reverse cycle (I) is negative. Therefore, the contact

Displacement Cycle (I)   Displacement Cycle (II)
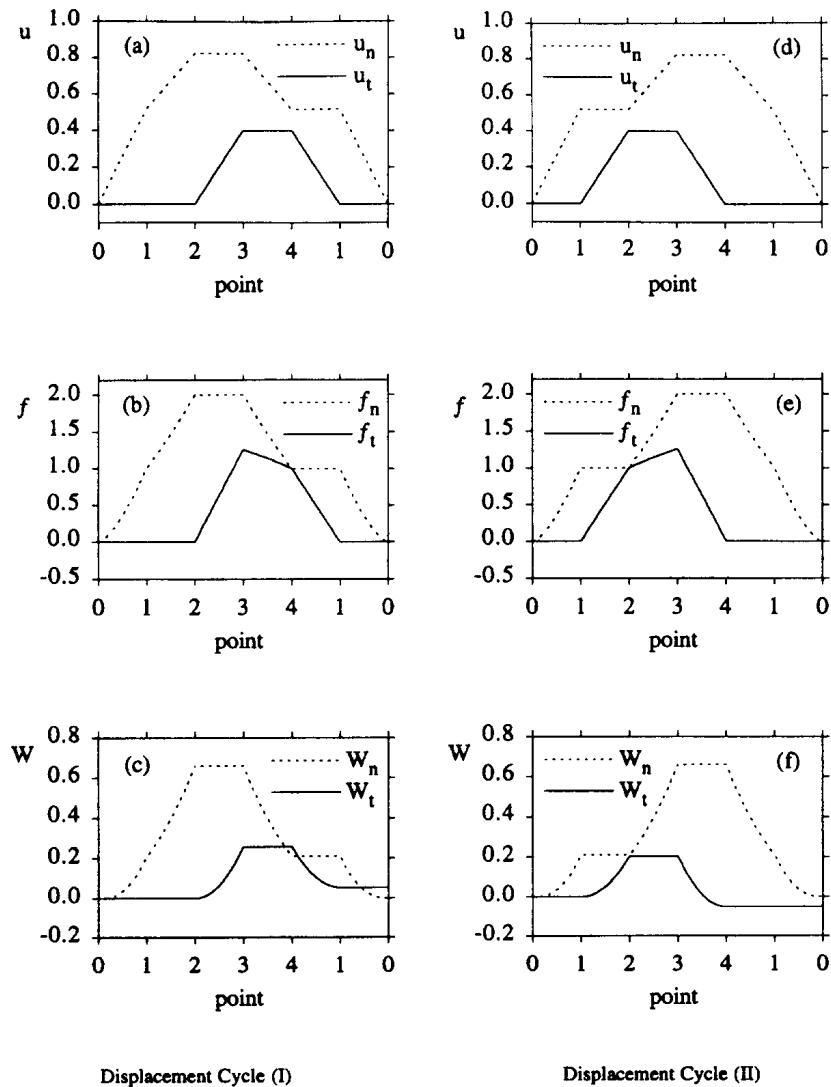
Fig. 5. The displacements, force, and external work associated with the displacement cycles and Eqs. (14)–(16). The displacements are normalized by R, the forces by $R^2\mu/(1 - \nu)$ and the work is normalized by $R^3\mu/(1 - \nu)$.

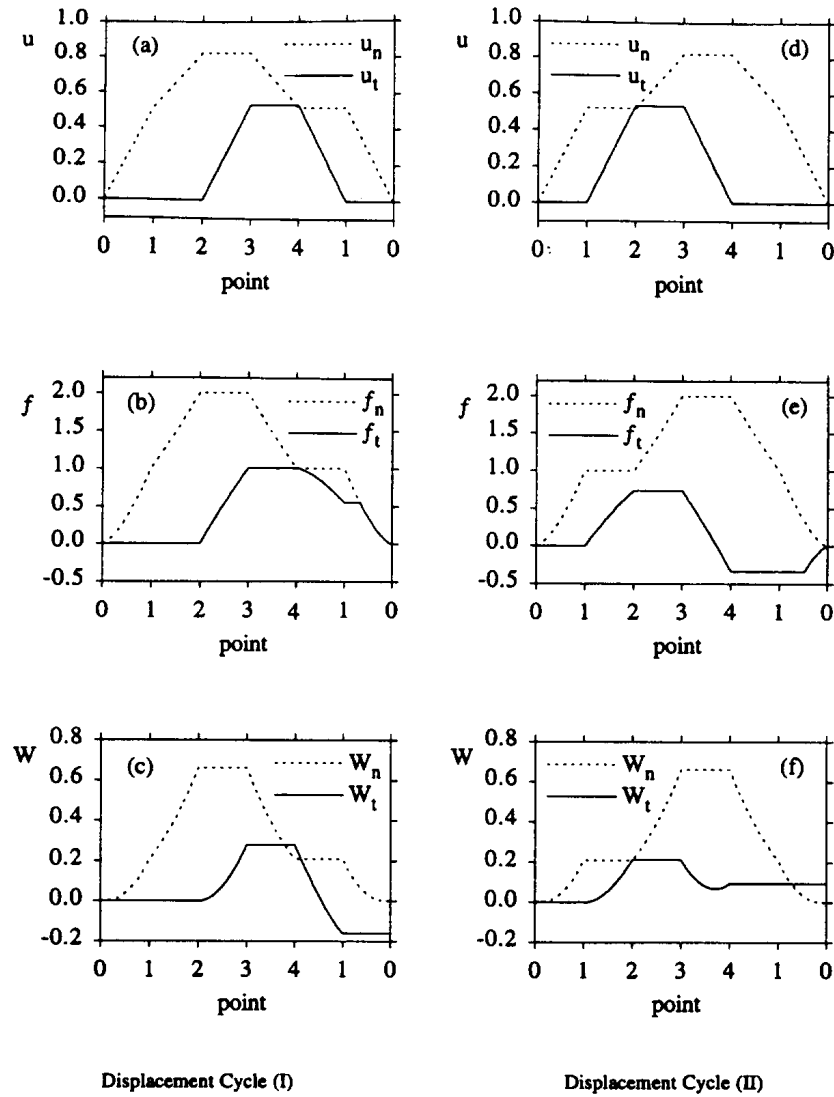Displacement Cycle (I)   Displacement Cycle (II)

Fig. 6. The displacements. force. and external work associated with the displacement cycles and Eqs. (18)–(20) (normalization as in Fig. 5).

force–displacement law (18)–(20) is also *thermodynamically inconsistent* in the sense that it also allows energy generation at no cost.

A different simplified contact force–displacement law that relates the tangential force to an *elastic* part of the tangential displacement was proposed by Walton (1995), and is presented here in a slightly different form

$$f_n = \tfrac{8}{3}\frac{\mu}{1-\nu}R^{1/2}u_n^{3/2},\tag{22}$$

$$f_t = 8\frac{\mu}{2-\nu}R^{1/2}u_n^{1/2}\left(u_t - u_t^p\right),\tag{23}$$

where u_t^p is the residual (i.e., plastic) contact dis-

placement when the tangential contact force is unloaded $(f_t = 0)$ while keeping the normal contact displacement u_n fixed. The value of u_t^p is determined by the evolution equation

$$\dot{u}_t^p = \tfrac{1}{2}\frac{\dot{u}_n}{u_n}\left(u_t - u_t^p\right)\quad\text{for }\dot{u}_n > 0,\tag{24}$$

where a superposed dot ('$\cdot$') denotes time rate of change, and it is further limited by the constraint function

$$g = \text{sign}\left(u_t - u_t^p\right)\left(u_t - u_t^p\right) - u_n\frac{\mu_f}{3}\frac{2-\nu}{1-\nu} \le 0.\tag{25}$$

Eq. (24) ensures that when the normal contact displacement u_n is increased while keeping the tangential contact displacement u_t fixed, the tangential contact force f_t remains unchanged. The constraint function (25) ensures that the tangential force does not exceed the friction limit

$$|f_t| \le f_n \, \mu_f. \tag{26}$$

The loading and unloading conditions resulting from the constraint (25) are given by the following evolution equation for u_t^p

$$\dot{u}_t^p = 0 \quad \text{for } (g < 0) \text{ or } (g = 0 \text{ and } \hat{g} \le 0), \tag{27a}$$

$$\dot{u}_t^p = \Gamma \quad \text{for } (g = 0 \text{ and } \hat{g} > 0), \tag{27b}$$

where

$$\hat{g} = \text{sign}(u_t - u_t^p)\dot{u}_t - \frac{\mu_f}{3}\frac{2 - \nu}{1 - \nu}\dot{u}_n, \tag{28}$$

$$\Gamma = \frac{\hat{g}}{\text{sign}(u_t - u_t^p)}. \tag{29}$$

Similar to Eq. (15) and in contrast to Eq. (19), Eq. (23) describes reduction of the tangential contact force as a result of decreasing normal contact displacement. However, similar to Eq. (19) and in contrast to Eq. (15), Eq. (23) does not describe an increase of the tangential contact force when the

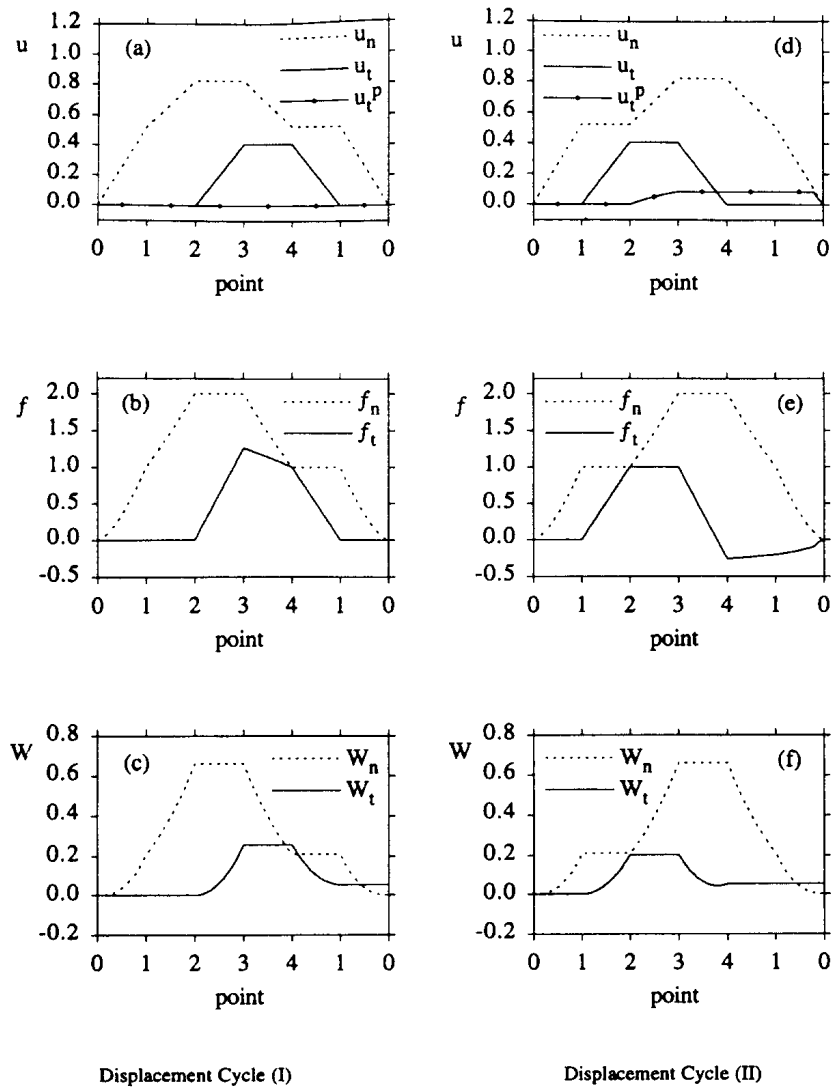Displacement Cycle (I)   Displacement Cycle (II)

Fig. 7. The displacements, force, and external work associated with the displacement cycles and Eqs. (22)–(29) (normalization as in Fig. 5).

normal contact displacement is increased and the tangential displacement is kept fixed. Accordingly, this contact force–displacement law eliminates the thermodynamical inconsistencies observed in Eqs. (15) and (19), and therefore appears to be physically reasonable.

To demonstrate consistency, consider the two load paths described in Fig. 4. The contact displacements, forces (22)–(25) and work done by these forces [Eqs. (24), (27a) and (27b) can be solved analytically for a given path], are illustrated in Fig. 7 for the arbitrary values [1],

$$\nu = 0.25,\tag{30a}$$

$$\mu_f = 1.0,\tag{30b}$$

$$u_{n1} = R(3/8)^{2/3},\tag{30c}$$

$$u_{n3} = R(3/4)^{2/3},\tag{30d}$$

$$u_{t3} = \frac{R}{8}\frac{2-\nu}{1-\nu}\frac{1}{\sqrt{u_{n1}}},\tag{30e}$$

which have been chosen to ensure that the condition in Eq. (27a) is satisfied whenever u_t is changing [i.e., the work done by the contact tangential force is unaffected by any slip arising from the constraint (25)]. In Fig. 7d, u_t^p increases in the path segment 2–3 due to increasing u_n according to Eq. (24) and decreases in the path segment 1–0 due to decreasing u_n according to Eq. (27b). Also, as can be seen in Fig. 7, both cycles begin and end in a stress free state and therefore, in both cycles no strain energy is stored in the spheres. For both cycles, the net work done by the normal force is zero, and in both cycles the net work done by the tangential force is greater than zero.

In order to prove that Eq. (23) is thermodynamically consistent, an arbitrary load cycle that begins and ends at $u_n = u_t = 0$ is considered next, and it is shown that the energy dissipation associated with this load cycle is not negative. For simplicity it is assumed that the condition in Eq. (27a) is satisfied whenever u_t is changing and that u_t^p is only controlled by the evolution equation (24) [the contact fictional slip described by the constraint (25) is trivially dissipative]. Also, for simplicity, it is assumed that along the load path u_n increases mono-

tonically between $u_n = 0$ and the maximal normal contact displacement u_{n1}, and that u_n decreases monotonically between u_{n1} and the end point ($u_n = 0$, $u_t = 0$). Accordingly, u_t and u_t^p are taken to be functions of u_n [i.e., $u_t = u_t(u_n)$, $u_t^p = u_t^p(u_n)$].

Along the load path between $u_n = 0$ and $u_n = u_{n1}$, Eq. (24) can be solved for u_t^p to give

$$u_t^p = u_n^{-1/2}\int_0^{u_n}\frac{u_t(x)}{2x^{1/2}}\,dx.\tag{31}$$

The work W_t done by the tangential force (23) during loading is given by

$$W_{t\,loading} = \int_0^{u_{n1}} f_t(x)u_t'(x)\,dx$$

$$= c\int_0^{u_{n1}}\left[u_t(x)x^{1/2}\right.$$

$$\left. -\int_0^x\frac{u_t(s)}{2s^{1/2}}\,ds\right]u_t'(x)\,dx,\tag{32a}$$

where $c = 8(\mu/2 - \nu)R^{1/2}$. Expanding the integrand of Eq. (32a) and integrating by parts yields

$$W_{t\,loading} = \frac{cu_{n1}^{1/2}u_{t1}^2}{2} - cu_{n1}^{1/2}u_{t1}u_{t1}^p + c\int_0^{u_{n1}}\frac{u_t^2(x)}{4x^{1/2}}\,dx.\tag{32b}$$

By using calculus of variations it can be shown that the maximum recoverable energy associated with the tangential force is obtained by decreasing u_t from $u_t = u_{t1}$ to $u_t = u_{t1}^p = u_t^p(u_{n1})$ while keeping the normal displacement fixed ($u_n = u_{n1}$), and then completely unloading u_n. Along this path the tangential force is given by

$$f_t = cu_{n1}^{1/2}(u_t - u_{t1}^p),\tag{33}$$

and the work associated with this force is given by

$$W_{t\,unloading} = \int_{u_{t1}}^{u_{t1}^p} f_t(u_t)\,du_t = -\frac{cu_{n1}^{1/2}}{2}(u_{t1} - u_{t1}^p)^2.\tag{34}$$

The net work done by the contact forces in the contact displacement cycle is therefore

$$W_{t\,net} = c\int_0^{u_{n1}}\frac{u_t^2(x)}{4x^{1/2}}\,dx - \frac{cu_{n1}^{1/2}}{2}(u_{t1}^p)^2.\tag{35}$$
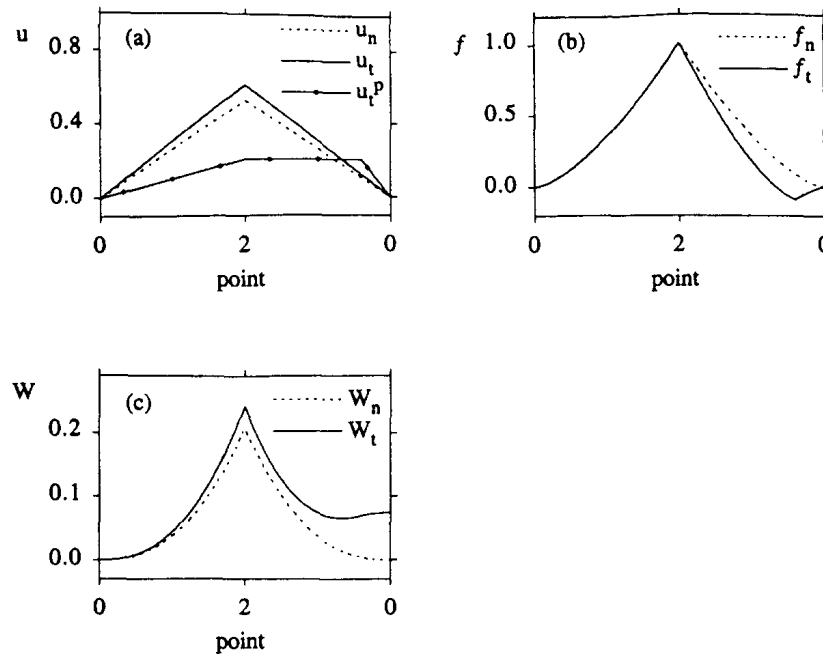
Fig. 8. The displacements, force, and external work associated with the load path (b) of Table 1 and Eqs. (22)–(29) (normalization as in Fig. 5).

The net work (35) satisfies the relations

$$W_{t\,net}(u_{n1} = 0, u_{t1} = 0) = 0, \tag{36a}$$

$$\frac{dW_{t\,net}}{du_{n1}} = \frac{c}{4u_{n1}^{1/2}}\left(u_{t1} - u_{n1}^{-1/2}\int_0^{u_{n1}} \frac{u_t(x)}{2x^{1/2}}dx\right)^2 \geq 0. \tag{36b}$$

The right hand side of Eq. (36b) vanishes only if the tangential displacement is constant $[\partial u_t(u_n)/\partial u_n = 0]$. Relations (36a) and (36b) ensure that the dissipated work $W_{t\,net}$ is always non-negative and therefore the simplified contact force–displacement law Eqs. (22)–(25) is thermodynamically consistent.

In this simplified contact law the current value of the scalar u_t^p replaces the detailed account of the load history previously mentioned. The thermodynamical consistency is maintained by *overestimating energy dissipation*. As an example, consider loading and unloading (retracing) along the path (b) described in Table 1. The contact displacements, forces Eqs. (22)–(25) and work done by these forces, are illustrated in Fig. 8 for the arbitrary values [1]

$$\nu = 0.25. \tag{37a}$$

$$\mu_f = 1.0. \tag{37b}$$

$$u_t = R\frac{2 - \nu}{1 - \nu}\frac{u_n}{2}, \tag{37c}$$

$$u_{n2} = R(3/8)^{2/3}. \tag{37d}$$

In the path segment 0–2, u_t^p increases proportionally to u_n according to Eq. (24). At the end of the path segment 2–0, u_t^p decreases due to a decrease of u_n according to Eq. (27b). In the loading segment 0–2, the normal and tangential contact forces have a fixed proportionality and are equal (in this specific problem) to the forces calculated by Walton (1987), but this proportionality is not maintained during the unload segment 2–0. In contrast to Walton's analytical solution of this problem, the simplified contact force–displacement law Eqs. (22)–(25) predicts energy dissipation as can be seen in Fig. 8c.

4. Discussion of macroscopic stress–strain relations

Granular materials are often modeled as a close random pack of identical spheres (Digby, 1981; Walton, 1987; Jenkins and Strack, 1993). By formulating a contact force–displacement law and using the

mean-field approximation, the macroscopic stress–strain relations may be derived. According to the mean-field approximation, displacement on the surface of a sphere relative to the sphere center is given by

$$u_i = Re_{ij}n_j, \quad (i, j = 1, 2, 3),$$ (38)

where u_i are the Cartesian components of the displacement, R is the radius of the sphere, e_{ij} are the Cartesian components of the macroscopic strain tensor, n_j are the Cartesian components of the (outward pointing) unit vector normal to the sphere surface, and the summation convention applies to repeated indices. Since Eq. (38) describes a homogeneous distortion, no relative roll or torsion will occur between neighboring spheres. With the mean-field approximation, the contact displacements can be determined for any arbitrary orientation of the contact. Then, the forces Eqs. (9) and (10) and stiffnesses Eqs. (11) and (12) may be averaged over all possible orientation of contacts (usually a uniform distribution over the unit sphere) to obtain the macroscopic stress–strain relation and macroscopic moduli-strain relation, respectively (Walton, 1987). Accordingly, the current state of stress will be history dependent but the current elastic moduli will depend only on the current state of deformation (Norris and Johnson, 1996). It is emphasized that the thermodynamic inconsistency of the simplified contact force–displacement laws previously mentioned does not 'average out' in the averaging process, and that macroscopic stress–strain relations based on inconsistent contact laws will be inconsistent (i.e., unphysical). Accordingly, if a simplified contact law is to be used in simulations of granular materials, it is important to choose a thermodynamically consistent one such as the contact law given by Eqs. (22)–(25).

The major deficiency of the mean-field approximation is that it does not ensure force and torque equilibrium of individual grains (when they are randomly packed), and thus renders predicted grain scale effects (e.g., changes in permeability, conductivity, etc.) meaningless. When the mean-field approximation is used nevertheless to motivate macroscopic stress–strain relations, it is sufficient to maintain a history of the macroscopic strain rather than maintaining the history of the contact displacement

for all individual contacts in the material. In this case, the exact contact force–displacement law described in Section 2 may be used without major difficulties (e.g., Johnson et al., 1996b).

The alternative to using the mean-field approximation is solving in detail the momentum equations (or equilibrium equations of the steady sate) for every individual grain. This demands that the possibility of relative roll and torsion between grains in contact be included in the contact force–displacement law.

5. Summary

The general contact force–displacement law described in Section 2 of this paper was derived analytically by integrating the differential form of the Hertz–Mindlin solution along the contact displacement path. The Hertz–Mindlin contact law (Mindlin, 1949) and the different contact law obtained by Walton (1978) are special cases of this general contact law. It was shown that the tangential contact traction depends on the loading history, and that decreasing normal contact displacements eliminate the influence of part of this history (Eq. (13)). It was also shown that slip does not necessarily occur when normal contact displacements are decreased.

Some simplified contact force–displacement laws proposed in the literature were shown to be thermodynamically inconsistent (i.e., unphysical) by demonstrating that they permit energy generation at no cost. A different simplified contact force–displacement law proposed by Walton (1995), in which the current value of a scalar u_t^p substitutes the detailed account of the load history, was shown to be thermodynamically consistent and therefore may be used to simulate the mechanical response of granular materials. However, it was shown that this contact force–displacement law has the characteristic that it overestimates energy dissipation.

When the mean-field approximation is used to calculate the mechanical response of random packs of spheres, the momentum equations of individual grains will not be satisfied. However, removing the mean-field approximation requires formulating elab-

orate contact force–displacement laws that include the possibility of relative roll and torsion between grains in contact. Nevertheless, when the mean-field approximation is used to motivate macroscopic stress–strain relations, it is sufficient to maintain a history of the macroscopic strain rather than maintaining the history of the contact displacement for all individual contacts in the material.

Acknowledgements

References

Chang, C.S., Y. Chang and M.G. Kabir (1992), Micromechanics modeling for stress–strain behavior of granular soils. I. Theory, J. Geotech. Eng. ASCE 118, 1959–1974.

Digby, P.J. (1981), The effective elastic moduli of porous granular rocks, ASME J. Appl. Mech. 48, 803–808.

Elata, D. (1996), On the oblique compression of two elastic spheres, ASME J. Appl. Mech., in press.

Jenkins, J.T. and O.D.L. Strack (1993), Mean-field inelastic behavior of random arrays of identical spheres, Mech. Mater. 16, 25–33.

Johnson, D.L. and A.N. Norris (1996a), Rough elastic spheres in contact: memory effects and the transverse force, J. Mech. Phys. Solids, in press.

Johnson, D.L., L.M. Schwartz, D. Elata, J.G. Berryman, B. Hornby and A.N. Norris (1996b), The effective elastic moduli of a random sphere pack: Stress induced anisotropy, Phys. Rev. E − Cond. Matter, submitted.

Johnson, K.L. (1985), Contact Mechanics, Cambridge University Press, Cambridge, UK.

Mindlin, R.D. (1949), Compliance of elastic bodies in contact, Trans. ASME 71, A-259.

Mindlin, R.D. and H. Deresiewicz (1953), Elastic spheres in contact under varying oblique forces, ASME J. Appl. Mech. 20, 327–344.

Norris, A.N. and D.L. Johnson, (1996), Nonlinear elasticity of granular media, ASME J. Appl. Mech., in press.

Walton, K. (1978), The oblique compression of two elastic spheres, J. Mech. Phys. Solids 26, 139–150.

Walton, K. (1987), The effective elastic moduli of a random packing of spheres, J. Mech. Phys. Solids 35, 213–226.

Walton, O. (1995), private communication.